ELSEVIER

Chemical Engineering Journal 78 (2000) 141–146

Chemical Engineering Journal

www.elsevier.com/locate/cej

The measurement of effective diffusivity for sulfur-tolerant methanation catalyst

Yu Guangsuo*, Yu Jianguo, Yu Zunhong

Institute of Clean Coal Technology, East China University of Science and Technology, 130 Meilong Road, Shanghai 200237, PR China

Received 9 November 1998; received in revised form 20 October 1999; accepted 22 October 1999

Abstract

The measurement of effective diffusivity for KD306 sulfur-tolerant methanation catalyst has been carried out using the 'single pellet string reactor' technique. The average tortuosity factor for KD306 catalyst was experimentally determined to be 7.2. The results of linearization method are in good agreement with the solutions of the parameter estimation method, which shows that the assumptions made in linearity processing are reasonable, and that the methods of linearization and parameter estimation can both be used to determine effective diffusivity efficiently.

Keywords: KD306 catalyst; Single pellet string reactor; Diffusivity

1. Introduction

Sulfur-tolerant catalyst plays an important role in the methanation of CO with H_2 and in making clean coal process technology feasible. The determination of effective diffusivity is needed to provide information for establishing the reaction–diffusion model for the catalyst.

The theoretical prediction of effective diffusivity of gases in porous catalysts is still not definitely resolved and in many cases not accurate enough. Among the reasons for this is that the diffusion flux may include contributions from several mechanisms, such as bulk, Knudsen and surface diffusion; and, in addition, a satisfactory geometric model for the pore structure is not yet available. Thus, an accurate estimation of effective diffusivity may have to be done experimentally.

Both steady-state and dynamic methods have been developed to measure the effective diffusivity in catalyst pores under inert conditions [1]. The commonly used steady state method, designed by Wicke and Kallenbach, suffers from the disadvantage that the mounting procedure may restrict access to pores and that diffusion reflects only those pores that allow passage of gas from one side of the pellet to the other. Dynamic methods have the advantage that the contributions of micropores and dead-ended pores are taken into account. The effective diffusivities measured by the dynamic methods, which more closely reflect diffusivities in a reacting system, are generally larger than those determined by steady state techniques.

Scott et al. [2] developed a single pellet string reactor (SPSR), the diameter of which is only slightly larger than those of pellets (ratios 1.1–1.4) and which contains 50 or more pellets to minimize axial dispersion. A large number of studies have since been reported using SPSR for diffusivity measurements [3–7].

In this work, the effective diffusivities of KD306 catalyst are measured under nonreacting conditions using a SPSR. A computer sampling system was developed to record the experimental data which employed four different pairs of tracer gas-carrier gas (He–N_2, N_2–He, Ar–N_2, N_2–Ar). The experimental results are processed by methods of linearization and parameter estimation.

2. Theory

For a gas pulse dispersion in SPSR, applying the Kubin–Kucera model [8], the moments of the broadened peak leaving the reactor are related to the parameters which are the axial dispersion coefficient E_A, the external mass transfer coefficient k_f, the adsorption equilibrium constant K_A, the adsorption rate constant k_{ads} and the intraparticle diffusivity D_{effA}. Moments of peaks appearing at the reactor outlet after injection of a square wave pulse of tracer gas of duration $t_0(\mu'_1, \mu_2)$ are sums of moments of the pulse response function $(\bar{\mu}'_1, \bar{\mu}_2)$, moments of the inlet square wave (μ'_{1s}, μ_{2s}) and moments corresponding to dead

* Corresponding author. Tel.: +86-21-6425-0192/2831; fax: +86-21-6425-0192.
E-mail address: zhyu@ecust.edu.cn (Y. Guangsuo)

1385-8947/00/$ – see front matter
PII: S1385-8947(00)00129-7

volumes (μ'_{1d}, μ_{2d}). The first absolute μ'_1 and second central μ_2 moments are, thus, given as

$$\mu'_1 = \bar{\mu}'_1 + \mu'_{1s} + \mu'_{1d} = \frac{L}{V}(1+\xi_0) + \frac{t_{0A}}{2} + \mu'_{1d} \quad (1)$$

$$\mu_2 = \bar{\mu}_2 + \mu_{2s} + \mu_{2d} = \frac{2L}{V}\left[\xi_1 + \frac{(E_A/\varepsilon)(1+\xi_0)^2}{V^2}\right] + \frac{t_{0A}^2}{12} + \mu_{2d} \quad (2)$$

where

$$\xi_0 = \frac{1-\varepsilon}{\varepsilon}\theta\left(1 + \frac{\rho_P K_A}{\theta}\right) \quad (3)$$

$$\xi_1 = \xi_a + \xi_i + \xi_e \quad (4)$$

$$\xi_a = \left(\frac{1-\varepsilon}{\varepsilon}\theta\right)\frac{\rho_P K_A}{\theta k_{ads}} \quad (5)$$

$$\xi_i = \left(\frac{1-\varepsilon}{\varepsilon}\theta\right)\frac{R^2\theta}{\gamma(\gamma+2)}\left(1+\rho_P\frac{K_A}{\theta}\right)^2\frac{1}{D_{effA}} \quad (6)$$

$$\xi_e = \left(\frac{1-\varepsilon}{\varepsilon}\theta\right)\frac{R^2\theta}{\gamma(\gamma+2)}\left(1+\rho_P\frac{K_A}{\theta}\right)^2\frac{\gamma+2}{k_f R} \quad (7)$$

The first absolute and second central moments of the chromatographic curve $C(t)$ are defined as

$$\mu_1 = \frac{m_1}{m_0} \quad (8)$$

$$\mu_2 = \frac{1}{m_0}\int_0^\infty (t-\mu_1)^2 C(t)\,dt \quad (9)$$

where the integrals m_0 and m_1 are given by

$$m_n = \int_0^\infty t^n C(t)\,dt \quad \text{for} \quad n = 0, 1 \quad (10)$$

3. Experimental

3.1. Apparatus and procedure

The experimental arrangements for SPSR are shown in Fig. 1. The apparatus consists of three parts, the gas supply and control part, the gas chromatographic column and the data collecting system. The tracer gas was injected into the carrier gas stream using a six-port injection valve with sample loop volume 0.2 ml. The column was mounted in a gas chromatograph oven where the temperature could be held constant within ±1 K. Column length was determined before the tube was coiled. 154 pellets of KD306 catalyst were packed into the column one by one. The inside diameter of the column was 6 mm and the length 0.668 m. Thermal conductivity detector, the signal of which was sent into a recorder, was used at the column outlet. Carrier gas flowrates were measured with soap-bubble flow-meter.

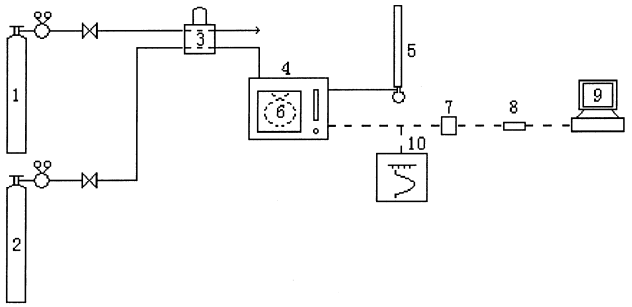

Fig. 1. Experimental apparatus for SPSR method. (1) tracer gas cylinder; (2) carrier gas cylinder; (3) six-port injection valve; (4) 102G gas chromatograph; (5) soap-bubble flow-meter; (6) SPSR; (7) transducer; (8) amplifier; (9) computer and (10) recorder.

A novel computer sampling system was developed to overcome experimental error caused by slow response of the recorder. The mV signal of the detector is amplified linearly into V signal by transducer and amplifier (ATP-M16), which can be recognized by computer sampling-board (ADC-30). The system, which assures wide-range-linearity and high-accuracy, responds briskly and could collect more than 50 data points per second.

After the catalysts were packed, the leakproofness was checked. Prior to experimental runs, the packed column was left over-night in the chromatograph oven at 423 K with inert carrier gas flowing. Experiments had been carried out at atmospheric pressure at 313, 353 and 383 K, with a carrier flow varying between 10 and 90 cm^3/min (Reynolds number 2–100). Each set of experiment had at least 15 data points and every data point was repeated no less than four times.

The experiments were divided into five groups: (a) impulse runs with Ar (carrier)–N_2 (tracer); (b) impulse runs with N_2–Ar; (c) adsorption runs with He–N_2; (d) inert runs with N_2–He and (e) blank runs with He–N_2, while the packed column with catalyst was replaced by a tube of diameter 0.3 mm.

4. Materials

The catalyst employed was obtained from University of Science and Technology of China, with reference number KD306. The cylindrical catalyst pellets (diameter= 5.422 mm, length=4.327 mm) were prepared by compressing particles. Pore size distribution (Fig. 2) was determined using a Micromeritics ASAP 2400 Sorptometer.

5. Experimental results

The computer signal H gained through sampling system is a linear amplification of the detector signal which is directly proportional to the tracer concentration C. Moments μ'_1, μ_2 are calculated from the computer signal H by Simpson formula according to the definition

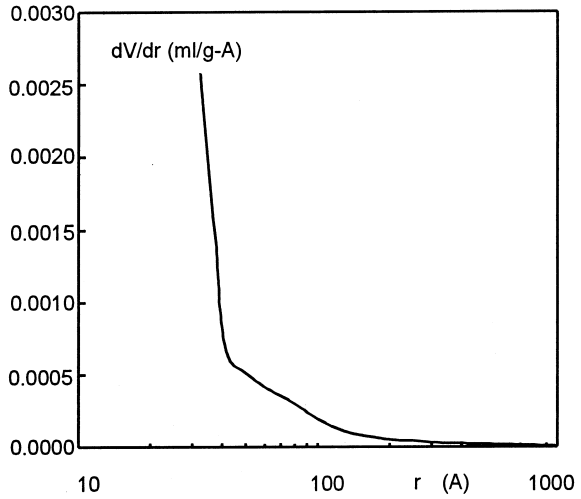

Fig. 2. Pore volume distribution for the pellet of KD306 catalyst.

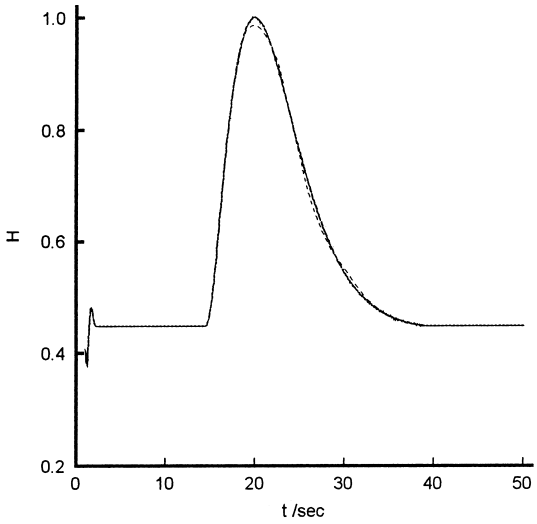

Fig. 3. A sample of experimental curve recorded by computer: N_2 (carrier gas)–Ar (tracer gas); temperature 383 K; superficial carrier gas velocity 27.75 cm/s; real curve — experimental signal and dotted curve — predicted results.

$$\mu_1' = \frac{\int_0^\infty tH(t)\,\mathrm{d}t}{\int_0^\infty H(t)\,\mathrm{d}t} \tag{11}$$

$$\mu_2 = \frac{\int_0^\infty (t-\mu_1')^2 H(t)\,\mathrm{d}t}{\int_0^\infty H(t)\,\mathrm{d}t} \tag{12}$$

A computer-recorded curve is shown in Fig. 3, and part of the experimental results are given in Table 1.

6. Results

6.1. Composite diffusivity D_{MA}

For diffusion of gases in porous catalyst particles, it is customary to define a tortuosity factor δ by the expression

$$D_{\mathrm{effA}} = \theta \frac{D_{\mathrm{MA}}}{\delta} \tag{13}$$

The effective diffusivity D_{effA} for component A, as evaluated from experimental data, is based upon the total pore plus solid area perpendicular to the direction of diffusion and on the most direct path, for example, the radial coordinate for a spherical particle. The composite diffusivity D_{MA} is a function of the pore radius r, if Knudsen diffusion is significant. The concentration of diffusing component within the pellet is always very low. Neglecting the composition effect and at constant pressure, D_{MA} [9] is given by

Table 1
N_2(carrier gas)–Ar(tracer gas) impulse runs

313 K			353 K			383 K		
V (cm/s)	μ_1' (s)	μ_2 (s^2)	V (cm/s)	μ_1' (s)	μ_2 (s^2)	V (cm/s)	μ_1' (s)	μ_2 (s^2)
8.01	84.86	174.24	7.84	74.92	109.08	5.89	81.06	115.30
10.08	70.23	135.16	9.33	62.87	95.76	8.47	66.75	88.90
12.12	57.13	103.33	9.83	59.30	81.75	10.47	54.86	68.67
15.01	45.24	83.73	12.29	50.40	68.47	12.45	45.93	55.74
17.99	40.12	72.19	13.35	45.63	61.45	13.64	43.16	50.75
19.99	36.49	70.40	15.67	39.89	52.15	15.33	38.89	44.87
20.61	35.67	66.59	16.61	36.57	46.87	16.44	36.43	43.23
23.42	31.29	62.14	17.99	34.54	43.43	17.54	33.86	40.41
24.93	30.33	61.38	19.97	31.38	39.21	19.58	30.21	33.82
27.45	27.99	50.57	23.06	27.15	33.33	23.00	26.32	29.01
29.63	25.67	45.75	24.79	25.28	30.66	24.17	24.88	27.12
31.59	25.02	43.63	27.43	23.40	29.02	27.27	22.67	24.00
31.90	24.77	42.95	29.43	21.73	25.95	27.75	22.26	23.67
32.84	24.04	40.38	31.58	20.51	24.44	29.41	21.12	22.59
33.77	22.88	37.08	32.33	20.06	23.13	32.19	19.04	20.67
36.35	21.82	35.67	33.92	19.16	21.74	34.32	18.05	19.14
37.24	21.31	34.64	35.62	18.01	22.08	36.46	16.92	18.42
39.07	20.05	31.48	38.55	16.91	19.38	39.18	16.00	17.15
41.98	17.72	29.13	39.40	16.16	17.85	40.41	15.61	16.00

Table 2
Composite diffusivity

Tracer gas	Carrier gas	D_{MA}		
		313 K	353 K	383 K
N_2	He	0.04498	0.04864	0.05124
He	N_2	0.09838	0.10809	0.11509
Ar	N_2	0.03019	0.03334	0.03559
N_2	Ar	0.03426	0.03797	0.04063

$$D_{MA} = \int_0^\infty \left(\frac{1}{D_{AB}} + \frac{1}{D_{KA}(r_P)} \right)^{-1} f(r_P)\, dr_P \quad (14)$$

where D_{AB} is the bulk diffusivity for the binary gas mixture A, B, and D_{KA} (r_p) is the Knudsen diffusivity for A in a pore of radius r_p.

The results of composite diffusivity D_{MA} obtained by applying the above model are summarized in Table 2.

6.2. Linearization method [10]

6.2.1. Adsorption equilibrium constant K_A

Under the condition that the value of adsorption equilibrium constant K_A is given, effective diffusivity D_{effA} could be evaluated from the correlation of D_{effA} with K_A in the item of intraparticle diffusion resistance. K_A is obtained by linear regression of the differences of the first absolute moments for adsorption runs and inert runs.

adsorption runs (He–N_2)

$$(\mu_1')_{ads} = (\bar{\mu}_1')_{ads} + (\mu_{1s}')_{ads} + (\mu_{1d}')_{ads} \quad (15)$$

inert runs (N_2–He)

$$(\mu_1')_{inert} = (\bar{\mu}_1')_{inert} + (\mu_{1s}')_{inert} + (\mu_{1d}')_{inert} \quad (16)$$

Subtracting Eq. (16) from Eq. (15)

$$\Delta\mu_1' = (\mu_1')_{ads} - (\mu_1')_{inert} = (\bar{\mu}_1')_{ads} - (\bar{\mu}_1')_{inert} = \frac{L}{V}\frac{1-\varepsilon}{\varepsilon}\rho_P K_A \quad (17)$$

$\Delta\mu_1'$ is correlated linearly with $1/V$, then K_A is obtained from the slope of the line (Table 3). The relation between the first absolute moments and the flow velocity of carrier gas for inert runs is regressed as a polynomial.

The low value of K_A in Table 3 shows that the adsorption of N_2 on KD306 catalyst is weak. The intercepts of the lines are not equal to 0, but the small deviations as shown in Table 3 manifest only slight error incurred in the experimentation.

Table 3
Adsorption equilibrium constant of tracing N_2

Temperature (K)	Intercept	Slope	Correlation coefficient	K_A (cm^3/g)
313	−0.1758	42.9548	0.80	0.06547
353	−0.1373	34.2844	0.75	0.05226
383	−0.3600	28.0333	0.90	0.04273

Table 4
Diffusion coefficients evaluated from the second central moments

Temperature (K)	Intercept	Slope	Correlation coefficient	E_A (cm^2/s)	D_{effA} (10^{-3} cm^2/s)	δ
313	3.3311	53.0989	0.93	2.3844	1.0681	7.10
353	2.2802	37.9516	0.98	1.9214	1.2484	6.57
383	1.7743	47.1057	1.00	2.6126	1.3428	6.43

6.2.2. Effective diffusivity D_{effA}

When particle size is increased, adsorption resistance decreases rapidly. External mass transfer resistance increases slightly, but it is still small and could be ignored. However, intraparticle diffusion resistance increases promptly and becomes the dominant contribution [2,5]. Based on the above assumptions, the second central moments for adsorption runs and blank runs could be deduced as follows:

$$(\mu_2)_{ads} = \frac{2L}{V}\left[\xi_i + \frac{(E_A/\varepsilon)(1+\xi_0)^2}{V^2}\right] + \frac{t_{0A}^2}{12} + \mu_{2d} \quad (18)$$

$$(\mu_2)_{blank} = \frac{t_{0A}^2}{12} + \mu_{2d} \quad (19)$$

If Eq. (19) is subtracted from Eq. (18), we obtain

$$(\mu_2)_{ads} - (\mu_2)_{blank} = \frac{2L}{V}\left[\xi_i + \frac{(E_A/\varepsilon)(1+\xi_0)^2}{V^2}\right] \quad (20)$$

$$\frac{\Delta\mu_2}{2L/V} = \xi_i + \frac{(E_A/\varepsilon)(1+\xi_0)^2}{V^2} \quad (21)$$

According to Eq. (21) a linear relation should exist between the second moment function on the left hand side and $1/V^2$. The data for different velocities are shown in Fig. 4 for 353 and 383 K. The lines represent the least square approximation of the data to Eq. (21). E_A could be gained from the slope, D_{effA} from the intercept. The relation between the second central moments and the flow velocity of carrier gas for blank runs is also regressed as a polynomial. The results obtained are summarized in Table 4, which contains the tortuosity factor δ. The results show that the values of δ at different temperatures are approximately consistent with each other, which indicates that δ depends only on the catalyst pore structure.

7. Parameter estimation method [5,11]

To assure the reliability of the parameter estimation method, the data taken for each set of experiment are no less than three times the number of parameters to be evaluated. The square sum of residuals is chosen as a criterion for the accuracy of the model.

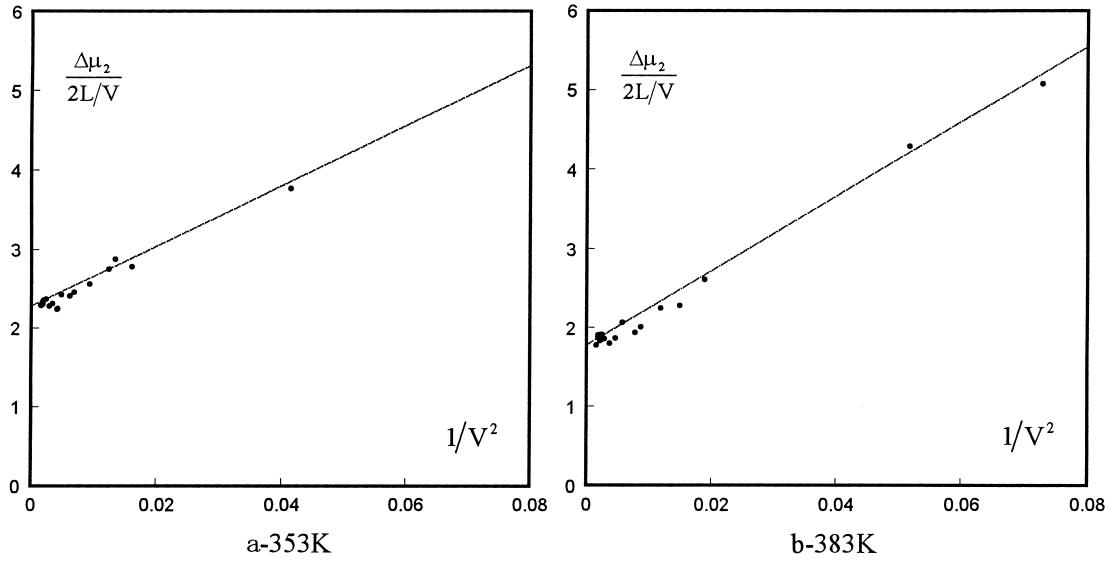

Fig. 4. $\Delta\mu_2/(2L/V)$–$1/V^2$ linear correlation.

$$f = \sum_{i=1}^{N}\{[(\mu_1')_i - (\mu_{1\text{cal}}')_i]^2 + [(\mu_2)_i - (\mu_{2\text{cal}})_i]^2\} \qquad (22)$$

where μ_1', μ_2 represent experimental values of the first absolute and second central moments, while $(\mu_1')_{\text{cal}}$, $(\mu_2)_{\text{cal}}$ are evaluated, respectively, by Eqs. (1) and (2).

The least square method of variable polyhedral algorithm [12] is employed to find the minimum value of f and the suitable value of D_{effA}. The other mass transfer parameters are obtained simultaneously. The results are shown in Tables 5–7.

In Table 5, the maximum deviation of δ from the average is about 18.5%, which shows once again that δ values are within a narrow range. Furthermore, δ values obtained from both methods as shown in Tables 4 and 5 are all clustered around an averaged δ of 7.2. From Table 7, it is easy to draw the conclusion that adsorption resistance and external mass transfer resistance could be neglected when compared with intraparticle diffusion resistance.

Table 5
Effective diffusivity of KD306 catalyst

Carrier gas	Tracer gas	Temperature (K)	D_{effA} (10^{-3} cm^2/s)	δ
He	N_2	313	1.1534	6.57
N_2	He	313	2.2043	7.52
He	N_2	353	1.3661	6.00
N_2	He	353	2.4043	7.58
He	N_2	383	1.4075	6.14
N_2	He	383	2.6188	7.41
Ar	N_2	313	0.7610	7.59
N_2	Ar	313	0.6536	7.78
Ar	N_2	353	0.7958	8.04
N_2	Ar	353	0.7173	7.83
Ar	N_2	383	0.8753	7.82
N_2	Ar	383	0.7363	8.15

Table 6
Estimation results of the other mass transfer parameters

Carrier gas	Tracer gas	Temperature (K)	K_A (cm^3/g)	E_A (cm^2/s)	k_{ads} (s^{-1})	k_f (cm/s)
He	N_2	313	0.06401	2.9522	5.6762	3.1477
He	N_2	353	0.05538	1.8382	6.9926	7.8007
He	N_2	383	0.04196	2.6467	4.6315	8.4569
Ar	N_2	313	0.09591	0.7225	3.4939	9.1181
N_2	Ar	313	0.10420	0.3613	1.8651	12.8058
N_2	Ar	353	0.07367	1.0964	4.5993	44.5733

Table 7
Resistance distribution

Carrier gas	Tracer gas	Temperature (K)	Adsorption resistance ξ_a/ξ_1 (%)	Intraparticle diffusion resistance ξ_i/ξ_1 (%)	External mass transfer resistance ξ_e/ξ_1 (%)
He	N_2	313	3.51	95.94	0.55
He	N_2	353	3.40	96.33	0.27
He	N_2	383	5.05	94.70	0.25

A sample of predicted curve obtained by the optimization method, based on the experimental curve and the model results of μ_1' and μ_2, is also shown in Fig. 3. The two curves are almost coincident with each other and the differences are very small.

8. Conclusions

The results of a linearization method are in good agreement with the solutions of the parameter estimation method, which shows that the assumptions made in linearity processing are reasonable and the methods of linearization and parameter estimation can both be used to determine effec-

tive diffusivity efficiently. The uniformity of the estimated values of δ also verifies the soundness of the SPSR method for measuring KD306 catalyst. The average tortuosity factor for KD306 catalyst was experimentally determined to be 7.2. The deviation of tortuosity factors obtained through Ar–N_2 as compared with that through He–N_2 is very slight, which suggests that Ar, instead of expensive He, might be used in the SPSR method.

9. Nomenclature

C	tracer concentration (mol/m^3)
D_{effA}	effective diffusivity (cm^2/s)
D_{MA}	composite diffusivity (cm^2/s)
E_{A}	axial dispersion coefficient (cm^2/s)
f	sum of residual squares defined by Eq. (22)
K_{A}	adsorption equilibrium constant (cm^3/g)
k_{ads}	adsorption rate constant (s^{-1})
k_{f}	external mass transfer coefficient (cm/s)
L	column length (cm)
R	mean radius of pellet (cm)
$t_{0\mathrm{A}}$	injection time of trace gas (s)
V	superficial carrier-gas velocity (cm/s)

Greek symbols

δ	tortuosity factor
ε	porosity of bed
γ	particle shape factor
μ_1'	first absolute moment (s)
μ_2	second central moment (s^2)
θ	porosity of particle
ρ_{p}	particle density (g/ml)
ξ_1	defined in Eq. (4)
ξ_{i}	intraparticle diffusion resistance defined in Eq. (6)
ξ_{e}	external mass transfer resistance defined in Eq. (7)
ξ_{a}	adsorption resistance defined in Eq. (5)

References

[1] W. Henry, J.R. Haynes, Catal. Rev.-Sci. Eng. 30 (4) (1988) 563–627.
[2] D.S. Scott, W. Lee, J. Papa, Chem. Eng. Sci. 29 (1974) 2155–2167.
[3] G.H.Y. Tang, D.L. Trimm, M.S. Wainwright, Chem. Eng. Aust. 12 (3) (1987) 9–12.
[4] R.K. Sharma, D.L. Cresswell, E.J. Newson, Ind. Eng. Chem. Res. 30 (1991) 1428–1433.
[5] A. Baiker, M. New, W. Richarz, Chem. Eng. Sci. 37 (4) (1982) 643–656.
[6] J. Valus, P. Schneider, Chem. Eng. Sci. 40 (8) (1985) 1457–1462.
[7] F. Garcia-Ochoa, A. Santos, Chem. Eng. Sci. 49 (18) (1994) 3091–3102.
[8] E.J. Kucera, J. Chromatography 19 (1965) 237–248.
[9] B.C. Zhu, Inorganic Chemical Reaction Engineering, Chemical Industry Press, Beijing, 1981 (in Chinese).
[10] N. Hashimoto, J.M. Smith, Ind. Eng. Chem. Fundam. 12 (3) (1973) 353–359.
[11] A.S. Chiang, A.G. Dixon, Y.H. Ma, Chem. Eng. Sci. 39 (10) (1984) 1461–1468.
[12] D.G. Liu, J.G. Fei, Y.J. Yu, et. al., FORTRAN Algorithm Assembly, National Defense Industry Press, Beijing, 1983 (in Chinese).